

Comparison of ITER performance predicted by semi-empirical and theory-based transport models

V. Mukhovatov¹, Y. Shimomura¹, A. Polevoi¹, M. Shimada¹,
M. Sugihara¹, G. Bateman², J.G. Cordey³, O. Kardaun⁴,
G. Pereverzev⁴, I. Voitsekhovich⁵, J. Weiland⁶, O. Zolotukhin⁷,
A. Chudnovskiy⁸, A.H. Kritiz², A. Kukushkin⁷, T. Onjun²,
A. Pankin² and F.W. Perkins⁹

¹ ITER International Team, ITER Naka Joint Work Site, Naka-machi, Naka-gun, Ibaraki-ken 311-0193, Japan

² Lehigh University, Bethlehem, PA 18015, USA

³ EURATOM-UKAEA Fusion Association, Culham Science Centre, Abingdon, UK

⁴ Association Euratom-IPP, MPI für Plasmaphysik, 2 Boltzmannstrasse, Garching, Germany

⁵ Equipe Turbulence Plasma, University of Provence, Marseilles, France

⁶ Chalmers University of Technology and EURATOM-NFR Association, Göteborg, Sweden

⁷ ITER International Team, ITER Garching Joint Work Site, Garching, Germany

⁸ Nuclear Fusion Institute, Russian Research Center 'Kurchatov Institute', Moscow, Russia

⁹ General Atomics 13-312, PO Box 85608, San Diego, CA 92186, USA

E-mail: mukhovv@itergps.naka.jaeri.go.jp

Received 13 November 2002, accepted for publication 20 June 2003

Published 28 August 2003

Online at stacks.iop.org/NF/43/942

Abstract

The values of $Q = (\text{fusion power})/(\text{auxiliary heating power})$ predicted for ITER by three different methods are compared. The first method utilizes an empirical confinement-time scaling and prescribed radial profiles of transport coefficients; the second approach extrapolates from specially designed ITER similarity experiments, and the third approach is based on partly theory-based transport models. The energy confinement time given by the ITERH-98(y, 2) scaling for an inductive scenario with a plasma current of 15 MA and a plasma density 15% below the Greenwald density is 3.7 s with one estimated technical standard deviation of $\pm 14\%$. This translates, in the first approach, for levels of helium removal, and impurity concentration, that, albeit rather stringent, are expected to be attainable, into an interval for Q of [6–15] at the auxiliary heating power, $P_{\text{aux}} = 40$ MW, and [6–30] at the minimum heating power satisfying a good confinement ELMy H-mode. All theoretical transport-model calculations have been performed for the plasma core only, whereas the pedestal temperatures were taken as estimated from empirical scalings. Predictions of similarity experiments from JET and of theory-based transport models that we have considered—Weiland, MMM, and IFS/PPPL—overlap with the prediction using the empirical confinement-time scaling within its estimated margin of uncertainty.

PACS numbers: 28.52.Av, 52.55.Fa, 52.25.Fi

1. Introduction

Predictions of the plasma performance in reactor scale devices are based largely on empirical global confinement scalings, whereas two other possible approaches, i.e. the dimensionless scaling analysis and application of theory-based transport models are used for comparison, as discussed in [1]. In this paper, we compare the performance of inductively driven

plasmas predicted by the three approaches for ITER taking into account recent progress in these areas.

2. Empirical scaling approach

A recent analysis of the enlarged global confinement database (ITERH.DB3) has confirmed the practical reliability of the ITER reference scaling ITERH-98P(y, 2) for thermal energy

confinement [1]:

$$\tau_{E,H98(y,2)} = 0.0562 I^{0.93} B^{0.15} \bar{n}_{19}^{0.41} P^{-0.69} R^{1.97} \kappa_a^{0.78} \varepsilon^{0.58} M^{0.19} \quad (1)$$

and one technical standard deviation was reduced from $\pm 18\%$ to $\pm 14\%$ leading to a 95% log non-linear interval estimate of $\pm 28\%$ [2, 3]. The scaling (1) satisfies the Kadomtsev constraint and is expressed in non-dimensional variables as

$$B \tau_{E,H98(y,2)} \propto (\rho^*)^{-2.7} \beta^{-0.9} (\nu^*)^{-0.01} q^{-3}, \quad (2)$$

where $\rho^* = \rho_i/a$, ρ_i is the toroidal ion Larmor radius, β is the normalized plasma pressure and ν^* is the normalized collisionality [1]. The point prediction for the thermal energy confinement time in ITER is $\tau_E = 3.7$ s at the following reference parameters: plasma current $I = 15$ MA, toroidal magnetic field $B = 5.3$ T, electron density (in 10^{19} m^{-3}) $\bar{n}_{19} = 10.1 = 0.85 n_G$ (where $n_G = I/(\pi a^2)$ is the Greenwald density), net heating power $P = 87$ MW, major plasma radius $R = 6.2$ m, elongation of plasma cross-section $\kappa_a \equiv V/(2\pi^2 R a^2) = 1.7$ with V being the plasma volume, $\varepsilon \equiv a/R = 0.32$, and average hydrogenic atomic mass $M = 2.5$ [4].

Figure 1 shows the fusion power P_{fus} and $Q = P_{\text{fus}}/P_{\text{aux}}$ plotted versus the confinement enhancement factor $H_{H98(y,2)} = \tau_E/\tau_{E,H98(y,2)}$ for the ITER inductive operating regime at the above reference parameters. These results are obtained with one-dimensional transport simulations using the 1.5D code ASTRA [5]. In the simulations, the scaling (1) is used for normalizing the transport coefficients in such a way that the energy confinement time computed by the code coincides with that given by the scaling relation. The value of P substituted into the scaling (1) is the total heating power P_{tot} corrected for the radiation inside the separatrix [4]:

$$P = P_{\text{tot}} - P_{\text{rad,eff}} = P_\alpha + P_{\text{oh}} + P_{\text{aux}} - \left(P_{\text{brem}} + P_{\text{cycl}} + \frac{P_{\text{line}}}{3} \right). \quad (3)$$

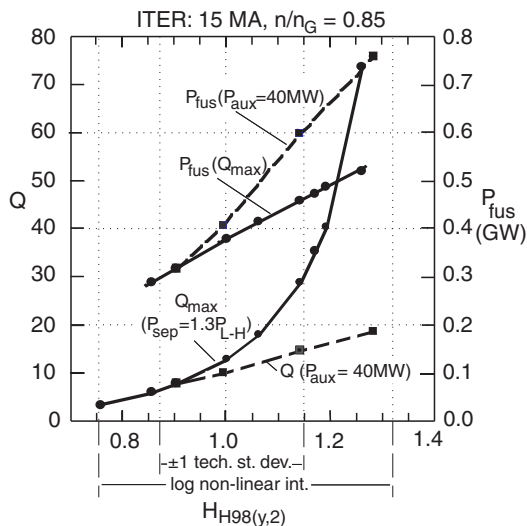


Figure 1. P_{fus} and Q at $P_{\text{aux}} = 40$ MW, and Q_{max} at $P_{\text{sep}} = 1.3 \times P_{L-H}$ versus $H_{H98(y,2)}$ predicted by the 1.5D ASTRA code with a one-dimensional transport-model based on ITERH-98P(y,2) scaling for the energy confinement time.

Here, $P_{\text{rad,eff}}$ is the effective radiation power, P_α the α -particle power, P_{oh} the Ohmic power, P_{aux} the auxiliary heating power, P_{brem} the bremsstrahlung power, P_{cycl} the cyclotron radiation power, and P_{line} is the line radiation power. Note that the power P in the confinement database used for obtaining the scaling (1) is not corrected for radiation power. Since the radiation power fraction in ITER is roughly similar to that in the present day machines, the adopted approach tends to be somewhat conservative for the prediction of ITER performance [6].

Radial profiles of the heat and particle diffusivities, χ_i , χ_e , D_e , D_{He} , and toroidal momentum diffusivity, χ_ϕ , are chosen in the form [7]

$$(\chi, D) = C_{\chi,D} f(\rho) h(\rho) + (1 - h(\rho)) \chi_i^{\text{neo}}, \quad (4)$$

where $C_{\chi,D}$ are numerical coefficients, $\rho = r/a$, $h(\rho) = 1$ for $\rho < 0.9$, and $h(\rho) = 0$ for $\rho > 0.9$ (corresponding to the reduction of the transport coefficients at the H-mode edge pedestal to the ion neoclassical level) and $f(\rho) = 1 + 3\rho^2$. It is assumed that $\chi_i = \chi_\phi = 2\chi_e$ and $D_e = D_{\text{He}} = \chi_e$.

The data shown satisfy the condition

$$P_{\text{sep}} \geq 1.3 \times P_{L-H}, \quad (5)$$

where P_{sep} is the power transported by the charged particles through the separatrix, $P_{\text{sep}} = P_{\text{tot}} - P_{\text{rad}}$, P_{rad} is the total power radiated from volume limited with the separatrix, and

$$P_{L-H} = 0.75 \bar{n}_{19}^{0.58} B^{0.82} R a^{0.81} M^{-1} \quad (6)$$

(MW, 10^{19} m^{-3} , T, m, amu)

is the power threshold for the L–H mode transition [8]. The scaling (6) gives $P_{L-H} = 49$ MW for parameters at the plasma burn phase when $P_{\text{tot}} = 121$ MW and $P_{\text{sep}} \approx 74$ MW. The ratio of P_{sep}/P_{L-H} (≈ 1.5 in the case considered) characterizes the margin in P_{sep} relative to the H–L back-transition neglecting a possible hysteresis in the H-mode power threshold. Equation (5) is in fact about 70% conservative for ITER conditions since the scaling (6) is not corrected for the radiative power loss, which amounted to an average of $\sim 30\%$ of the heating power in the threshold database. The radiation power ($\sim 40\%$ of P_{tot}) is subtracted to estimate P_{sep} in ITER. This margin in P_{L-H} is close to the uncertainty in the P_{L-H} projection for ITER [1, 8, 9]. Note that the ITER design provides an opportunity to apply a P_{aux} as high as 73 MW during the initial stage of ITER operation and up to 110 MW during the later operational stage [4]. In the inductive high- Q scenario considered here, the L–H mode transition is planned for an early phase of the discharge when the plasma density is lower ($\sim 4 \times 10^{19} \text{ m}^{-3}$), reducing P_{L-H} to ≈ 28 MW. Therefore, ITER will be equipped to cope with a higher P_{L-H} within the uncertainty of the threshold scaling and, to some extent, also of the confinement scaling, though at the price of reducing Q .

While 2% of Be and 0.12% of Ar ions are assumed to be present in the plasma, the He content is calculated self-consistently assuming $\tau_{\text{He}}^*/\tau_E = 5$ where $\tau_{\text{He}}^* = \tau_{\text{He}}/(1 - R_{\text{He}})$, τ_{He} is the intrinsic particle confinement time for He nuclei, and R_{He} is the effective He recycling coefficient. Simulations show that at $P_{\text{aux}} = 40$ MW the value of Q increases with $H_{H98(y,2)}$ as $H_{H98(y,2)}^{\xi_H}$ with $\xi_H \approx 3$, and the minimum value of $H_{H98(y,2)}$ satisfying equation (5) is ≈ 0.83 giving $Q \approx 5.8$.

Since Q increases with reducing P_{aux} , the maximum Q is achieved at the lowest P_{aux} compatible with equation (5), i.e. at $P = 1.3P_{L-H}$. Q_{max} is a stronger function of $H_{H98(y,2)}$ (compared to Q at $P_{\text{aux}} = 40$ MW) with the exponent ξ_H of about 5 in the vicinity of $H_{H98(y,2)} = 1$. The interval $[0.87, 1.15]$ of $H_{H98(y,2)}$ associated with one standard deviation in ITERH-98P(y,2) scaling prediction, and the log non-linear interval $[0.76, 1.32]$ translate into Q_{max} intervals of $[6, 30]$ and $[3.5, >80]$, and Q intervals at $P_{\text{aux}} \geq 40$ MW of $[6, 15]$ and $[3.5, 20]$, respectively. The sensitivity of Q to other parameters of interest, expressed in terms of the exponent ξ_y in the relation $Q \propto Y^{\xi_y}$ (Y denotes parameters I, n, \dots), in the vicinity of the reference operating point is as follows: $\xi_I \approx 3.4$ for the plasma current at $B = \text{const.}$ and $\langle n_e \rangle / n_G = \text{const.}$; $\xi_n \approx 1.6$ for the plasma density at $I = \text{const.}$; and $\xi_{DT} \approx 2.2$ ($\xi_{DT} \approx 6$ at $P_{\text{tot}} = P_\alpha + P_{\text{aux}} = \text{const.}$) for the DT ion fraction, varying with the τ_{He}^* / τ_E ratio.

The log non-linear interval for $H_{H98(y,2)}$ is assumed to cover uncertainties in the ITER performance predictions with the limitations of the power law form of the scaling (1) and with effects of parameters not included in this scaling explicitly, such as the density peaking factor $\langle n_e \rangle / n_{\text{ped}}$ (n_{ped} is the density at the top of the edge pedestal), closeness to the density limit characterized by the ratio $\langle n_e \rangle / n_G$, and the plasma triangularity δ . Corrections to the scaling (1), i.e. ancillary scalings of $H_{H98(y,2)}$ factor, were suggested in [10] (based on JET only data) and in [3] (based on the ITERH.DB3v10 database). For ITER with $\delta = 0.5$ and $\langle n_e \rangle / n_G = 0.85$, this correction gives $H_{H98(y,2)} = 1.03$ at a moderately peaked density with $n_{\text{ped}} / \langle n \rangle = 0.71$ as observed in present day experiments [11] and can be expected in ITER at an appropriate combination of gas puffing and pellet fuelling [12, 13]. The most unfavourable value here, $H_{H98(y,2)} = 0.82$, is predicted for ITER plasma with $n_{\text{ped}} / \langle n \rangle = 1$, which is slightly outside one technical standard deviation but well inside the log non-linear interval. The offset non-linear two-term scaling suggested in [14] and the analysis in [2] predict relatively low τ_E , i.e. $H_{H98(y,2)} \approx 0.80$ and 0.85 , respectively, whereas the two-term scalings suggested in [15], e.g. the thermal conduction model and the MHD model, predict $H_{H98(y,2)}$ very close to 1 although with strongly different relative contributions from the core and pedestal terms. In [16], we can see that the sum of two power laws leads (on a logarithmic scale) to a positive curvature of the density dependence, instead of a negative one, which is needed to describe a roll-over effect near the Greenwald density.

The above data correspond to moderately conservative assumptions used in the ITER project documentation [4]. Recent measurements of the spectral profile of a He I spectral line in the divertor region of JT-60U [17] suggest that there is a possibility of improving the efficiency of helium ash exhaust due to the elastic collisions of He atoms with D/T ions. The B2/Eirene code simulations show that this effect can provide a significant (factor of 3–5) reduction of helium concentration at the separatrix in ITER [18]. This effect deserves careful experimental verification. Figure 2 illustrates the importance of reducing the He content for maximizing Q . These results are obtained by $\frac{1}{2}$ -D analysis, described in [2], based on a prescribed temperature profile shape, and ITER equilibrium profiles. It was assumed in this analysis that 2% of Be,

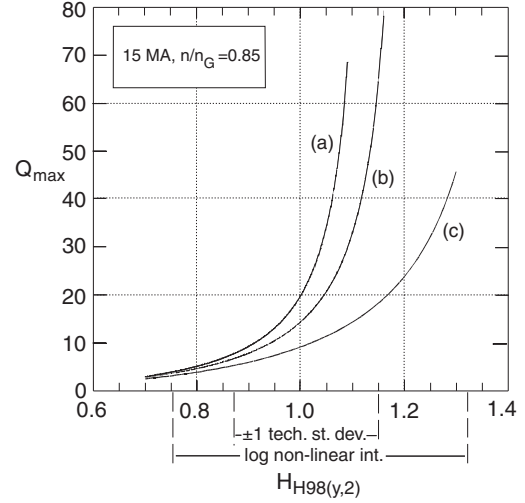


Figure 2. Q_{max} versus $H_{H98(y,2)}$ at different values of the He content, predicted by the $\frac{1}{2}$ -D ITINT1.SAS code at $P_{\text{sep}} \geq P_{L-H}$, (see [2], figure 3). The curves (a), (b), and (c) correspond to τ_{He}^* / τ_E of 2.5, 5, and 10, which provide, at $H_{H98(y,2)} = 1$, the helium fractions f_{He} , of 1.6%, 3.2%, and 5.8%, respectively.

0.5% of C, 0.5% of O, and 1% of H ions are present in the plasma. One can see that reduction of f_{He} from 3.2% (the reference case) to 1.6%, increases Q_{max} to 20 at $H_{H98(y,2)} = 1$, and the margin in $H_{H98(y,2)}$ for achieving $Q_{\text{max}} = 10$ to approximately 0.1. Furthermore, figure 2 suggests a possibility of achieving $Q > 50$ within uncertainty of predictions.

3. Dimensionless scaling approach

The dimensionless scaling approach is based on Kadomtsev's principle, which says that confinement scalings can be expressed in a non-dimensional form [1]:

$$B\tau_E = (\rho^*)^{-(2+\alpha_\rho)} F\left(\beta, v^*, q, \frac{R}{a}, \kappa, \delta, \dots\right), \quad (7)$$

where $\alpha_\rho = 0$ and 1 correspond to Bohm and gyroBohm scaling, respectively. The parameter α_ρ was measured in a number of tokamak experiments and found to be close to 1 in low- q ($q_{95} \sim 3-4$) ELMy H-mode discharges. In particular, $\alpha_\rho \approx 1.15$ was obtained in DIII-D [19, 20] and $\alpha_\rho \approx 0.7$ in JET [21]. Note that the latter value coincides with that in the dimensionless form of the ITERH-98P(y, 2) confinement scaling (equation (2)). Equation (7) permits the scaling of the product $B\tau_E$ from present day machines to larger devices by decreasing ρ^* while keeping other non-dimensional parameters fixed.

Let us consider a 'JET-like ITER', which is a machine with $B = 5.3$ T and $a = 2$ m, the same as in the ITER design, and with dimensionless parameters $\beta, v^*, q_{95}, R/a, \kappa_x$, and δ_x the same as in a specified JET shot. Under these conditions, some other parameters of the JET-like ITER can be expressed through the ratios $b = B/B_{\text{JET}}$ and $r = a/a_{\text{JET}}$ and the relevant JET parameters as follows: $\rho^* = b^{-2/3} r^{-2/3} \rho_{\text{JET}}^*$, $W_{\text{th}} = b^2 r^3 W_{\text{th, JET}}$, $I = br I_{\text{JET}}$, $\langle n_e \rangle = b^{4/3} r^{-1/3} \langle n_e \rangle_{\text{JET}}$, $\langle n_e \rangle / n_G = b^{1/3} r^{2/3} \langle n_e \rangle / n_{G, \text{JET}}$. The values P_{fus} and $P_{\text{rad, eff}}$ in JET-like ITER cannot be easily obtained in this way, therefore,

Table 1. Parameters of JET DT pulse #42983 and non-dimensionally extrapolated JET-like ITER discharge. ITER design parameters are shown for comparison.

Parameter	JET #42983	JET-like ITER	ITER design
B (T)	3.46	5.3	5.3
a/R (m/m)	0.96/2.89	2.0/6.0	2.0/6.2
κ_x/κ_a	1.75/1.6	1.75/1.6	1.85/1.74
δ_x	0.23	0.23	0.48
q_{95}	2.77	2.77	3.0
$\beta_{N,th}$	1.46	1.46	1.63
ν^*	0.05	0.05	0.023
Z_{eff}	2.7	2.7	1.67
$B\tau_E$ (T s)	1.76	20–30	19.6
τ_E (s)	0.51	3.74–5.6	3.7
W_{th} (MJ)	12.5	265	320
P (MW)	24.5	71–47	87
$P_{rad,eff}$ (MW)		28	34
P_{tot} (MW)		99–76	121
P_{fus} (MW)		275	400
P_{aux} (MW)	24.5	44–21	40
Q		6.2–13.3	10
I (MA)	4.47	14.3	15
$\langle n_{e20} \rangle$ (m^{-3})	0.81	1.12	1.01
$H_{H98(y,2)}$	0.98	0.99–1.12	1.0
$\langle n_e \rangle/n_G$	0.55	0.99	0.85

they have been estimated using similar values calculated for ITER design parameters. In particular, the fusion power in JET-like ITER has been obtained from the relation $P_{fus} = (W_{th}/W_{th,ITER})^2 P_{fus,ITER}$.

An example of such extrapolation (by a factor of 2.45 in ρ^*) from a JET DT pulse #42983 [22] to a JET-like ITER is shown in table 1. The ITER design parameters are shown in the last column of the table. One can see that the value of $B\tau_E$ predicted for the JET-like ITER is ≈ 20 Ts at $\alpha_\rho = 0.7$ and ≈ 30 Ts at $\alpha_\rho = 1.15$. The extrapolated value of W_{th} (thermal plasma energy) is 265 MJ resulting in a Q of 13.3 and 6.2 for α_ρ of 1.15 and 0.7, respectively. The case with $Q = 6.2$ satisfies equation (5) while P is slightly below P_{L-H} at $Q \approx 13.3$. To make the latter case compatible with equation (5), P_{aux} must be increased, which will increase, to a smaller extent, P_{fus} and reduce Q to ≈ 10 .

Although this JET pulse looks like a relevant one, a number of its dimensionless parameters, i.e. $\beta_{N,th} = 1.46$ and $\delta = 0.23$, deviate significantly from ITER. Therefore, discharges with a better match to the dimensionless ITER parameters and a more accurate measurement of the parameter α_ρ are needed to improve the accuracy of this extrapolation. According to the analysis of these similarity experiments, the dependence of $B\tau_E$ on β is very weak, i.e. $B\tau_E \propto \beta^{0.03}$ in DIII-D [19, 20] and $B\tau_E \propto \beta^{-0.05}$ in JET [21], which is in clear contradiction to the dimensionless form of the global confinement scaling (equation (2)). The reasons for this discrepancy are not yet well understood.

4. Theory-based model predictions

In this section, the values of Q and P_{fus} predicted for ITER by four theory-based transport models, i.e. the multi-mode (MM) [23], Weiland [24], IFS/PPPL [25] and GLF23 [26] are compared. All four models utilize transport driven by the drift wave turbulence, although a detailed

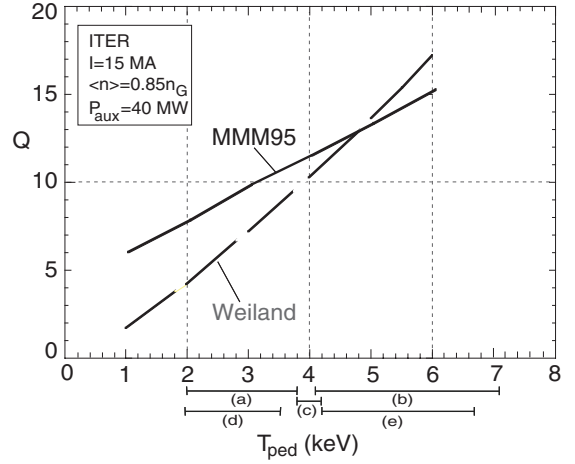


Figure 3. Q versus T_{ped} given by MM (MMM95) and Weiland models. The horizontal bars at the bottom show the ranges of T_{ped} predicted by edge pedestal models (a) and (b) [15], (c) [31], (d) [11], and (e) [32].

treatment of the physics of micro-instabilities is somewhat different. The IFS/PPPL model and the related, more complete GLF23 model, are based on non-linear gyro-fluid turbulence simulations for the amplitude of the ion-temperature-gradient (ITG) mode together with linear gyro-kinetic computations for the threshold of this mode. Transport obtained in this way is higher than that predicted by the more advanced non-linear gyro-kinetic turbulence simulations [27], and the GLF23 model tends to underpredict experimental thermal energy at higher edge temperatures for ASDEX Upgrade [28]. The Weiland reactive drift wave model, which provides the ITG and trapped electron mode (TEM) part of the MM model, comes close to agreeing with the results of the non-linear gyro-kinetic simulations [27, 29]. In addition, electromagnetic effects in the Weiland model have been developed to treat finite beta effects. The MM model also includes transport due to resistive and kinetic ballooning modes and neoclassical transport.

The values of Q versus T_{ped} predicted for ITER by the Weiland [30] and MM models (T_{ped} is the ion temperature at the top of the edge pedestal, $r_{ped} = 0.95a$) are shown in figure 3. Both models show an increase in Q with T_{ped} , $Q \propto (T_{ped})^\gamma$ with $\gamma \approx 1.25$ for the Weiland model and $\gamma \approx 0.5$ for the MM model. The different sensitivity of Q to changes in T_{ped} is usually attributed to a different ‘stiffness’ of the temperature profile, i.e. different rate of increase in transport above the critical temperature gradient. For the models under discussion this seems to be not the case since the major part of transport (i.e. that associated with ITG and TE modes) is essentially the same in both models. The difference in γ can be, at least partially, due to the difference in input parameters. In particular, Z_{eff} is 15% smaller and the He content is about two times smaller in MMM simulations. Also, the auxiliary heating was applied predominantly to ions ($P_{aux,i} \approx 1.5 \times P_{aux,e}$) in the MMM case, while $P_{aux,i} \approx P_{aux,e}$ was assumed in the Weiland case.

According to these simulations ITER will need $T_{ped} = 3.0$ – 3.9 keV to obtain $Q = 10$ at $I = 15$ MA and $P_{aux} = 40$ MW. The horizontal bars at the bottom of the figure show approximate ranges of T_{ped} predicted for ITER by the five

pedestal scalings listed in table 2. It is assumed that the density at the top of the edge pedestal follows the scaling $n_{\text{ped}} = 0.7\langle n \rangle$ [11]. The scalings (a), (c), (d), and (e) are based on the assumption that the critical pressure gradient $(dp/dr)_{\text{cr}}$ in the pedestal is determined by the MHD stability limit caused by the ballooning and/or peeling modes with the pedestal width Δ_{ped} being a function of plasma parameters, e.g. the ion Larmor radius ρ_i and magnetic shear s , or the poloidal beta β_p and plasma size R . Theory-motivated dependences are compared with data from individual H-mode discharges or from the pedestal database to determine the numerical coefficient. The scaling $\Delta_{\text{ped}} \propto \rho_i s^2$ in combination with the ideal ballooning mode limit for $(dp/dr)_{\text{cr}}$ after normalization to JET discharges gives for ITER $T_{\text{ped}} = 3.5\text{--}4.5\text{ keV}$ (scaling (c)) [31]. In [11], a similar pedestal model was used together with the MM transport-model applied for the plasma core (scaling (d)). Since the value of Δ_{ped} is needed to compute q , s , and $(dp/dr)_{\text{cr}}$, and since Δ_{ped} is a function of T_{ped} , a non-linear equation solver was used to determine T_{ped} resulting, for ITER, in $T_{\text{ped}} \approx 3.2\text{ keV}$ at $r_{\text{ped}} = 0.95a$. A similar value of T_{ped} (2.9 keV) is predicted for ITER by the MHD limit model with $\Delta_{\text{ped}} \propto \rho_i^\alpha R^{1-\alpha}$ fitted to the pedestal database DB3v2 without Type III ELMs [15] (scaling (a)). Allowing an explicit dependence of $(dp/dr)_{\text{cr}}$ on plasma elongation, triangularity and aspect ratio, with fitting to the pedestal data from ASDEX Upgrade, JET and JT-60U, results in scaling that predicts for ITER significantly higher pedestal temperature, $T_{\text{ped}} = 5.3\text{ keV}$ [32] (scaling (e)). This scaling, however, does not fit pedestal data from DIII-D and C-Mod, possibly because of different physical conditions, i.e. the plasma edge in the second stable regime for ballooning modes in DIII-D and ELM-free H-mode in C-Mod. All experimental data used for obtaining and checking the scaling (e) have been taken from the International pedestal database [33]. The highest point prediction for T_{ped} in ITER, i.e. 5.6 keV, is given by the thermal conduction model assuming that the dominant loss term in the pedestal is the thermal conduction term [15] (scaling (b)). Earlier versions of this scaling [16, 34] predict even higher values of T_{ped} for ITER ($\sim 6.5\text{ keV}$). On the other hand, there are pedestal models predicting very narrow barrier widths and, hence, low pedestal temperatures, $T_{\text{ped}} \sim 1\text{--}2\text{ keV}$, for ITER, e.g. a model based on the turbulence suppression by the flow velocity shear, associated with the ion loss on orbits crossing the separatrix [35]. These models, however, have a worse fit to the available experimental data compared to the scalings discussed above [36]. For simplicity, the RMSE of fit of the scalings to the pedestal database is taken here to express the relative uncertainty between the various T_{ped} projections to ITER shown in table 2 and figure 3. To estimate the confidence interval of T_{ped} in ITER, a statistical error propagation, as described in [6], is needed.

Table 2. T_{ped} predicted for ITER by different pedestal scalings.

Pedestal scaling	T_{ped} (keV)
(a) Cordey <i>et al</i> [15]	$2.9 \pm 31\%$
(b) Cordey <i>et al</i> [15]	$5.6 \pm 27.1\%$
(c) Sugihara <i>et al</i> [31]	3.5–4.5
(d) Kritz <i>et al</i> [11]	$2.74 \pm 32\%$
(e) Sugihara <i>et al</i> [32]	$5.3 \pm 26\%$

To evaluate the uncertainties in the (partly) theory-based model predictions for ITER we run the models at the same input parameters and the same boundary conditions using the 1.5D transport code ASTRA [5]. The following simplified approach [37] was employed in the simulations. In the transport models, only diagonal terms of the turbulent transport matrix were retained. Heat diffusivities for electrons and ions were taken directly from the transport models whereas the particle flux was taken as $\Gamma = v^{\text{neo}} n_e - (D_e^{\text{neo}} + D_e^{\text{an}}) \nabla n_e$ with D_e^{neo} and v^{neo} being the neoclassical diffusion coefficient and pinch velocity, respectively. The anomalous diffusion coefficient is taken to be $D_e^{\text{an}} = 0.2(\chi_e^{\text{an}} + \chi_i^{\text{an}})$.

Figure 4 compares the ITER fusion powers predicted by ASTRA simulations using the Weiland, IFS/PPPL and GLF23 models [37]. The DT ion fraction, $f_{\text{DT}} = 0.94$, was fixed in these calculations. One can see that the IFS/PPPL and GLF23 models predict significantly lower P_{fus} at given T_{ped} than the Weiland model. P_{fus} increases with T_{ped} as $P_{\text{fus}} \propto (T_{\text{ped}})^\gamma$ with $\gamma \approx 1.25$ for the Weiland model and $\gamma \approx 2$ for the IFS/PPPL and GLF23 models. The minimum values of the pedestal temperature, 4.7 keV, and 5.3 keV, required, respectively, by the IFS/PPPL and GLF23 models for obtaining $Q = 10$ at $P_{\text{aux}} = 40\text{ MW}$, are higher than that required by the Weiland model ($\approx 3\text{ keV}$ in this series of calculations). All three models predict a possibility of reaching ignition in ITER, i.e. plasma sustained by α -particle heating only ($P_{\text{aux}} = 0$), at sufficiently high $T_{\text{ped}} \geq (4.5\text{--}6.5)\text{ keV}$ (parts of dashed curves above $P_{\text{fus}} \approx 500\text{ MW}$ in figure 4).

A large scatter in Q and P_{fus} values at $T_{\text{ped}} = \text{const.}$, seen in figures 3 and 4, could be taken as a measure of the uncertainty in the prediction of core plasma parameters in ITER using the transport models considered. The prediction capability of these models is weakened further by a large uncertainty in the prediction of T_{ped} . Nevertheless the above results allow the conclusion that the range of Q predicted for ITER by the theory-based transport models, using the presently available, possible range of T_{ped} projections, overlaps with those given by the two models based on empirical confinement scaling and dimensionless analysis.

Figure 5 shows T_i , T_e , and n_e profiles in ITER at $Q \approx 10$ predicted by transport simulations using the MM model,

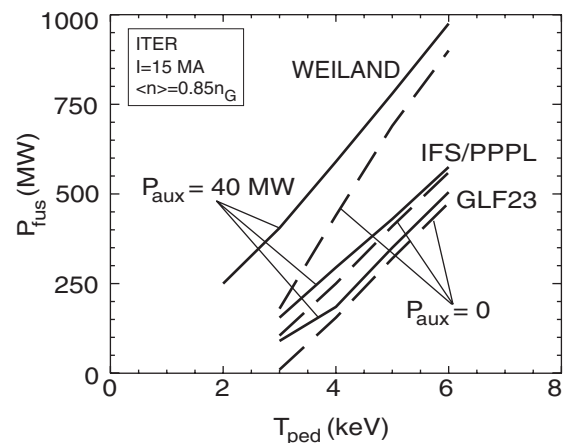


Figure 4. P_{fus} versus T_{ped} predicted for ITER by the simplified Weiland, IFS/PPPL and GLF23 models incorporated into the ASTRA code [37], at $P_{\text{aux}} = 40\text{ MW}$ (—) and $P_{\text{aux}} = 0$ (- - -). $f_{\text{DT}} = 0.94$ was fixed in these simulations.

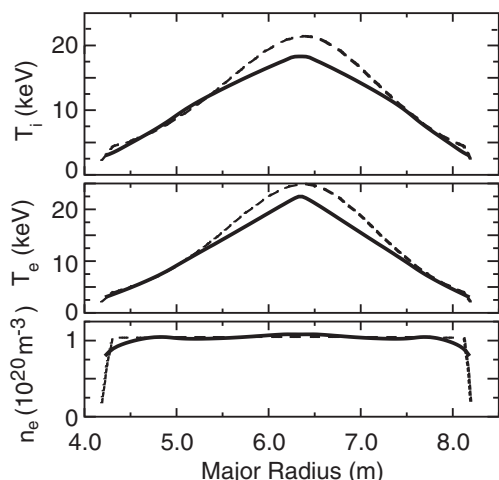


Figure 5. Radial profiles of T_i , T_e and n_e predicted by MMM with $T_{ped} = 2.74$ keV at $r/a = 1$ (—) and by the model based on the empirical scaling (1) (---) for ITER with $I = 15$ MA, $\langle n_e \rangle / n_G = 0.84$, and $P_{aux} = 40$ MW.

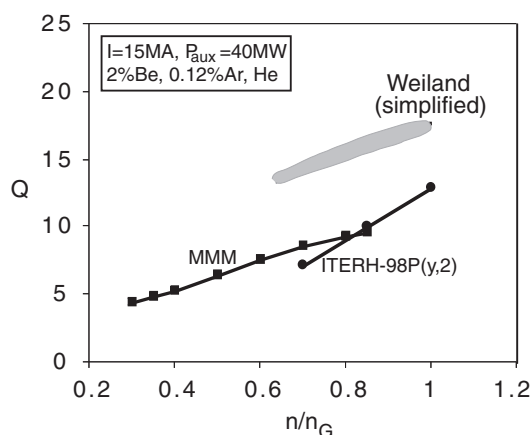


Figure 6. Q versus $\langle n_e \rangle / n_G$ predicted for ITER by MM and simplified Weiland models with two different scalings for T_{ped} . Also shown is Q dependence on $\langle n_e \rangle / n_G$ based on ITERH-98P(y, 2) confinement scaling.

with $T_{ped} \approx 2.7$ keV, given by the pedestal model based on magnetic and flow shear stabilization (solid curves) [11]. In these simulations the top of the edge pedestal was located at $r/a = 1$. Also shown in this figure are the temperature and density profiles obtained in ASTRA simulations using empirical scaling (1) [4, 7] (dashed curves). The same major input parameters, $I = 15$ MA, $\langle n_e \rangle / n_G = 0.85$ and $P_{aux} = 40$ MW, and the averaged impurity concentrations of 2% Be and 0.12% Ar were used in both simulations. However, the central He and Ar concentrations in the MMM case were lower than in simulations with scaling (1), resulting in a higher central DT ion fraction. This explains the nearly equal fusion powers (423 and 410 MW) obtained in these simulations, although the central ion temperature obtained in the MMM simulation is lower.

Figure 6 shows Q versus $\langle n_e \rangle / n_G$ for three cases, assuming $n_{ped} = 0.7 \langle n_e \rangle$. The MMM and simplified Weiland model results are obtained using two different pedestal

models described in [11] and [15], respectively. Both curves demonstrate a similar, relatively weak dependence of Q on plasma density in the $\langle n_e \rangle / n_G$ range of 0.6–1, although with Q values diverging by a factor of 2. The dependence of Q on $\langle n_e \rangle / n_G$ based on the ITERH-98P(y, 2) scaling is stronger, and Q values at $\langle n_e \rangle / n_G \sim 0.85$ are close to those given by the MM model. All available scalings for the edge pedestal show an increase in T_{ped} with the plasma current, $T_{ped} \propto I^\gamma$ with γ in the range of 0.58 [32] to 2 [11, 31]. A scan with plasma current, at $T_{ped} = \text{const.}$ and $\langle n_e \rangle / n_G = \text{const.}$ gives $Q \propto I^{\xi_1}$ with $\xi_1 = 2.3$ for the MM model, which becomes $\xi_1 = 3.0$ –4.8, taking into account the above T_{ped} scalings with I . Note that $\xi_1 = 3.4$ given by the scaling (1) is within this range.

5. Summary

The possibility of achieving high Q (≥ 10) in ITER predicted by the transport-model based on the ITERH-98P(y, 2) confinement scaling is reasonably well confirmed by the dimensionless scaling analysis as well as by the (partly) theory-based transport modelling. Reduction of He concentration predicted by the B2/Eirene code, if realized, will significantly increase the operational window for $Q = 10$. The dimensionless scaling projection from the JET DT pulse #42983 to the ITER reference inductive regime yields $Q = 6$ –13, which is compatible with predictions based on the global confinement scaling. According to the MM, Weiland, IFS/PPPL and GLF23 theory-based transport models, the pedestal temperatures, T_{ped} , at $r/a = 0.95$ required for achieving $Q = 10$ in ITER are 3.2 keV, 3.9 keV, 4.7 keV, and 5.3 keV, respectively. These values of T_{ped} are within the presently available, large possibility range of T_{ped} projections. A more accurate model of the edge pedestal and of its self-consistent coupling to the core plasma is required. Further elaboration and testing of theory-based transport models is needed in order to select the most reliable ones for a more accurate prediction of the ITER performance.

Acknowledgments

This report was prepared as an account of work undertaken within the framework of ITER Transitional Agreements (ITA). These are conducted by the Participants: Canada, China, the European Atomic Energy Community, Japan, Korea, the Russian Federation, and the United States of America, under the auspices of the International Atomic Energy Agency. The views and opinions expressed herein do not necessarily reflect those of the Participants to the ITA, the IAEA of any agency thereof. Dissemination of the information in this paper is governed by the applicable terms of the former ITER EDA Agreement. VM wishes to thank Dr A.E. Costley and Dr B. Green for fruitful discussions and comments. OK acknowledges discussion with Dr G. Becker.

References

- [1] ITER Physics Basis 1999 *Nucl. Fusion* **39** 2175
- [2] Kardaun O. 2002 *Nucl. Fusion* **42** 841

- [3] Kardaun O.J.W.F. 2002 Interval estimate of the global energy confinement time during ELMy H-mode in ITER-FEAT, based on the international multi-tokamak ITERH.DB3 dataset *IPP-IR-2002/5-1.1 Report* Max-Planck-Institut für Plasmaphysik, Garching and <http://www.ipp.mpg.de/ipp/netreports>
- [4] ITER Technical Basis 2002 *ITER EDA Documentation Series* No. 24, (Vienna: IAEA) chapter 4
- [5] Pereverzev G.V. and Yushmanov P.N. 2002 ASTRA Automated System for Transport Analysis in a Tokamak *IPP Report 5/98*, Max-Planck-Institut für Plasmaphysik, Garching
- [6] Kardaun O. 1999 *Plasma Phys. Control. Fusion* **41** 429
- [7] Polevoi A.R. *et al* 2002 *J. Plasma Fusion Res. Series* **5** 82
- [8] Snipes J.A. *et al* 2000 *Plasma Phys. Control. Fusion* **42** A299
- [9] ITER Confinement Database and Modeling Expert Group (presented by T. Takizuka) 1997 *Proc. 16th Int. Conf. on Fusion Energy (Montreal 1996)* vol 2 (Vienna: IAEA) p 795
- [10] Cordey J.G. *et al* 2002 *Plasma Phys. Control Fusion* **44** 1929
- [11] Kritz A.H. *et al* 2002 *Proc. 29th EPS Conf. on Controlled Fusion and Plasma Physics (Montreux, 2002)* vol 26B (ECA) D-5.001
- [12] Lang P.T. *et al* 2000 *Nucl. Fusion* **40** 245
- [13] Polevoi A.R., Medvedev S.Yu., Pustovitov V.D., Mukhovatov V.S., Shimada M., Ivanov A.A., Poshekhonov Yu.Yu. and Chu M.S. 2002 Possibility of $Q > 5$ stable, steady-state operation in ITER with moderate β_N and H-factor *Proc. 19th Int. Conf. on Fusion Energy (Lyon, 2002)* paper CT/P-08 <http://www.iaea.org/programmes/ripc/physics/fec2002/html/node170.htm/>
- [14] Takizuka T. 1998 *Plasma Phys. Control. Fusion* **40** 851
- [15] Cordey J.G. for the ITPA H-Mode Database Working Group and ITPA Pedestal Database Working Group 2003 *Nucl. Fusion* **43** 669
- [16] Kardaun O.J.W.F. for the International Confinement Database Working Group 2001 *Proc. 18th Int. Conf. on Fusion Energy (Sorrento, 2000)* (Vienna: IAEA) CD-ROM file ITERP/4, <http://www.iaea.org/programmes/ripc/physics/fec2000/pdf/iterp.04.pdf>
- [17] Kubo H. *et al* 1999 *Plasma Phys. Control. Fusion* **41** 747
- [18] Kukushkin A. *et al* 2002 *Plasma Phys. Control. Fusion* **44** 931
- [19] Petty C.C. *et al* 1998 *Nucl. Fusion* **38** 1183
- [20] Petti C.C. *et al* 1998 *Phys. Plasmas* **5** 1695
- [21] JET Team (presented by J.G. Cordey) 1997 *Proc. 16th Int. Conf. on Fusion Energy (Montreal, 1996)* vol 1 (Vienna: IAEA) p 603
- [22] Horton L.D. *et al* 1999 *Nucl. Fusion* **39** 993
- [23] Bateman G. *et al* 1998 *Phys. Plasmas* **5** 1793
- [24] Nordman H. *et al* 1999 *Nucl. Fusion* **39** 1157
- [25] Kotschenreuther M. *et al* 1995 *Phys. Plasmas* **2** 2381
- [26] Waltz R.E. *et al* 1997 *Phys. Plasmas* **4** 2482
- [27] Dimits A.M. *et al* 2000 *Phys. Plasmas* **7** 969
- [28] Tardini G. *et al* 2002 *Nucl. Fusion* **42** 258
- [29] Ross D.V. and Dorland W. 2002 *Phys. Plasmas* **9** 5031
- [30] Weiland J. 2001 *28th Eur. Phys. Soc. Conf. on Controlled Fusion and Plasma Physics (Funchal, Madeira, 18–22 June 2001)* vol 25A (ECA) (Geneva: European Physics Society) CD-Rom Paper P2.039, <http://epsppd.epfl.ch/Madeira/html/pdf/P2.039>
- [31] Sugihara M. *et al* 2000 *Nucl. Fusion* **40** 1743
- [32] Sugihara M., Mukhovatov V., Polevoi A. and Shimada M. MHD model based scaling for H-mode edge pedestal pressure in tokamaks *Plasma Phys. Control. Fusion* at press
- [33] Hatae T. *et al* 2001 *Nucl. Fusion* **41** 285
- [34] Thomsen K. *et al* 2002 *Plasma Phys. Control. Fusion* **44** A249
- [35] Osborne T.H. *et al* 2002 Characteristics of the H-Mode pedestal and extrapolation to ITER *Proc. 19th Int. Conf. on Fusion Energy (Lyon, 2002)* paper CT-03 <http://www.iaea.org/programmes/ripc/physics/fec2002/html/node52.htm>
- [36] Onjun T. *et al* 2002 *Phys. Plasmas* **9** 5018
- [37] Pereverzev G.V. *et al* 2002 *29th EPS Conf. on Controlled Fusion and Plasma Physics (Montreux, 2002)* vol 26B (ECA) (Geneva: European Physical Society) CD-Rom Paper P-1.072, http://elise.epfl.ch/pdf/P1_072.pdf